Numerical simulation of coupled state-to-state kinetics and heat transfer in viscous non-equilibrium flows

O. Kunova' , E. Kustova' , M. Mekhonoshina' , and G. Shoev'

Citation: **1786**, 070012 (2016); doi: 10.1063/1.4967588
View online: http://dx.doi.org/10.1063/1.4967588
View Table of Contents: http://aip.scitation.org/toc/apc/1786/1
Published by the American Institute of Physics

Numerical Simulation of Coupled State-to-State Kinetics and Heat Transfer in Viscous Non-Equilibrium Flows

O. Kunova[1,a)], E. Kustova[1,b)], M. Mekhonoshina[1,c)] and G. Shoev[1,2,3,d)]

[1]*Saint Petersburg State University, 7/9 Universitetskaya nab., St. Petersburg 199034, Russia*
[2]*Khristianovich Institute of Theoretical and Applied Mechanics SB RAS, 4/1 Institutskaya str., Novosibirsk 630090, Russia*
[3]*Novosibirsk State University, 2 Pirogova Str., Novosibirsk, 630090, Russia*

[a)]kunova.olga@gmail.com
[b)]elena_kustova@mail.ru
[c)]mekhonoshinama@gmail.com
[d)]shoev@itam.nsc.ru

Abstract. The influence of vibrational-dissociation kinetics on mass and heat transfer in non-equilibrium flows of N_2/N and O_2/O mixtures behind shock waves is investigated on the basis of the state-to-state approach. A method of the numerical solution of coupled equations of gas dynamics and state-to-state kinetics in the commercial flow solver ANSYS Fluent is proposed. Based on the proposed numerical tool, the flows near a cone and behind a planar shock wave are studied. The calculation results are compared with available experimental data.

INTRODUCTION

Modeling of non-equilibrium flows and prediction of flow parameters, mass and heat transfer are important for many practical problems of gas dynamics. Many studies of state-to-state vibrational-chemical kinetics have been performed since the 1960s. Due to high computational difficulties, the majority of investigations deal 1D inviscid flows such as flows behind shock waves [1, 2], in nozzles [3, 4], in a boundary layer [5, 6], and simple 2D flows [7]. In recent years the state-to-state model was extended for simulation of more complex rotational-vibrational relaxation [8, 9] and vibration-electronic-radiation kinetics [10, 11]. Furthermore, the state-to-state approach was applied recently to estimate transport properties in a 2D low-temperature flow around a blunt body [12].

In the present paper, we study the non-equilibrium kinetics, diffusion and heat transfer behind shock waves in hypersonic flows of binary mixtures $N_2(i)$/N and $O_2(i)$/O. The state-to-state kinetic theory approach [13] is used for calculating vibrational distributions, gas dynamic parameters, and transport properties in the relaxation zone behind the shock front for different flow conditions.

The calculation algorithm for state-dependent transport coefficients developed within the framework of the kinetic theory [14, 13] requires solving transport linear systems for all vibrational states at each step of the numerical simulation. This procedure is very complicated and resource-consuming. A simplified algorithm for calculating diffusion and energy transfer was developed in [15] and applied in our earlier works [16, 17]. The simplified way is based on the task splitting procedure: first, modeling of the inviscid flow in the Euler approximation is carried out and, then, the total energy flux and diffusion fluxes are calculated by using post-processing of data obtained at the first step. While providing a tool for qualitative estimates of heat and mass transfer in strongly non-equilibrium flows, such an approach cannot be applied for accurate heat flux assessment.

The objective of the present work is a self-consistent study of the effects of state-dependent transport phenomena in non-equilibrium flows on the basis of the state-to-state kinetic theory. This paper continues the work performed in [18], where the method of computations was suggested for inviscid flows within the framework of the state-to-state approach. Fully coupled equations of fluid mechanics and state-to-state kinetics are numerically solved in the commercial flow solver ANSYS Fluent. In recent years, this commercial flow solver has been widely used to simulate

30th International Symposium on Rarefied Gas Dynamics
AIP Conf. Proc. 1786, 070012-1–070012-8; doi: 10.1063/1.4967588
Published by AIP Publishing. 978-0-7354-1448-8/$30.00

high-enthalpy non-equilibrium flows in the two-temperature approximation. The influence of vibrational relaxation on perturbations in a shock layer on a flat plate was studied in [19]. An attempt to validate different vibrational relaxation models was made in [20] on the basis of comparisons of the shock wave location near a plate and the shock stand-off distance near a cone. Simulations of chemically reacting flows were performed in [21, 22] in order to validate different dissociation models. The effect of surface catalycity on the surface heat flux was studied in [23, 24]. In the present work, numerical algorithms of the state-to-state kinetics and transport coefficients evaluation are implemented into the commercial flow solver through the user-defined functions. The implemented algorithms are used for simulations of 1D and 2D binary mixture flows behind shock waves.

KINETIC SCHEME AND FLOW EQUATIONS

In the present work, we study high-temperature flows of binary mixtures $N_2(i)$/N and $O_2(i)$/O behind shock waves. The scheme of non-equilibrium kinetic processes in the relaxation zone includes state-specific reactions of dissociation

$$A_2(i) + M \rightarrow A + A + M, \quad M = A_2,\ A, \tag{1}$$

and VT (TV) exchanges of vibrational and translational energies

$$A_2(i) + M \leftrightarrow A_2(i \pm 1) + M, \quad M = A_2,\ A. \tag{2}$$

Here $A_2(i)$ is a diatomic molecule at the vibrational level i and M is an inert collision partner. Note that in our research we consider only single-quantum exchanges, which are much more probable than multi-quantum transitions. Since the dominating process in the shock heated gas is TV vibrational excitation, in our calculations we do not take into account VV transitions of vibrational energy between molecules. Moreover, estimates carried out for inviscid gas show a weak influence of VV exchanges on gasdynamic parameters [11].

Governing Equations

The master equations for vibrational and chemical relaxation of the considered mixture can be written in the form

$$\frac{\partial n_i}{\partial t} + \nabla \cdot (n_i \mathbf{v}) + \nabla \cdot (n_i \mathbf{V}_i) = R_i^{VT} + R_i^{dis}, \quad i = 1, \ldots l, \tag{3}$$

$$\frac{\partial n_a}{\partial t} + \nabla \cdot (n_a \mathbf{v}) + \nabla \cdot (n_a \mathbf{V}_a) = -2 \sum_i R_i^{dis}, \tag{4}$$

and coupled to the conservation equations of mass, momentum, and total energy

$$\frac{\partial \rho}{\partial t} + \nabla \cdot (\rho \mathbf{v}) = 0, \tag{5}$$

$$\frac{\partial \rho \mathbf{v}}{\partial t} + \nabla \cdot (\rho \mathbf{v}\mathbf{v}) + \nabla \cdot \mathbf{P} = 0, \tag{6}$$

$$\rho \frac{\partial E}{\partial t} + \rho \mathbf{v} \cdot \nabla E + \nabla \cdot \mathbf{q} + \mathbf{P} : \nabla \mathbf{v} = 0. \tag{7}$$

In Eqs. (3)-(7), n_i is the ith level population, l is the total number of excited levels, $\mathbf{v}$ is the gas velocity, E is the total energy per unit mass

$$\rho E = \frac{3}{2} n k_B T + \rho_m E_{rot} + \sum_i \varepsilon_i n_i + \varepsilon_a n_a,$$

$\rho = n_m m_m + n_a m_a = \rho_m + \rho_a$ and $n = n_m + n_a$ are the mass and number densities of the gas mixture, m_m and m_a are the molecular and atomic masses, n_a and n_m are the atom and molecule number densities, k_B is the Boltzmann constant, T is the translational-rotational temperature, E_{rot} is the rotational energy per unit mass, ε_i is the vibrational energy of a molecule at the ith vibrational level, ε_a is the formation energy of atoms, $\mathbf{V}_i$ is the diffusion velocity of molecules at the ith vibrational level, $\mathbf{V}_a$ is the diffusion velocity of atoms, $\mathbf{q}$ is the total energy flux, $\mathbf{P}$ is the pressure tensor. In the calculations, the vibrational energies are simulated by the harmonic oscillator model with $l = 32$ for N_2 and $l = 25$ for O_2.

The production terms in equations (3) and (4) describe the changes in the vibrational level populations and atom number density due to the non-equilibrium kinetic processes (1) and (2):

$$R_i^{VT} = \sum_{\mathrm{M}} n_{\mathrm{M}} \sum_{i'=i\pm1} \left(n_{i'} k_{i'i}^{\mathrm{M}} - n_i k_{ii'}^{\mathrm{M}} \right), \tag{8}$$

$$R_i^{dis} = -\sum_{\mathrm{M}} n_{\mathrm{M}} n_i k_{i,dis}^{\mathrm{M}}, \quad \mathrm{M} = m,\ a. \tag{9}$$

The source terms (8) and (9) contain state-specific rate coefficients $k_{ii'}^{\mathrm{m}}$, $k_{ii'}^{\mathrm{a}}$, $k_{i,dis}^{\mathrm{m}}$, $k_{i,dis}^{\mathrm{a}}$ for vibrational energy transitions (2) and dissociation (1) in collision with molecules and atoms (denoted by the superscripts "m" and "a", respectively). Recombination is neglected since its effect in shock heated flows is weak.

Diffusion Velocities and Total Energy Flux

For the state-to-state approach, the expressions for the diffusion velocities, total energy flux, and pressure tensor were derived in [13, 14, 15]. The viscous stress tensor can be represented in the form

$$\mathbf{P} = (p - p_{rel})\mathbf{I} - 2\eta\mathbf{S} - \zeta\nabla\cdot\mathbf{v}\mathbf{I}, \tag{10}$$

p is the mixture pressure, p_{rel} is the relaxation pressure, η and ζ are the coefficients of shear and bulk viscosity, and $\mathbf{S}$ and $\mathbf{I}$ are the deformation rate and unit tensors.

The diffusion velocities and total energy flux can be written as a sum of contributions of different processes [25]:

$$\mathbf{V}_i = \mathbf{V}_i^{TD} + \mathbf{V}_i^{MD} + \mathbf{V}_i^{DVE}, \quad \mathbf{V}_a = \mathbf{V}_a^{TD} + \mathbf{V}_a^{MD}, \tag{11}$$

$$\mathbf{q} = \mathbf{q}^{HC} + \mathbf{q}^{MD} + \mathbf{q}^{TD} + \mathbf{q}^{DVE}. \tag{12}$$

Here $\mathbf{V}_i^{MD}$, $\mathbf{V}_a^{MD}$, $\mathbf{V}_i^{TD}$, $\mathbf{V}_a^{TD}$, and $\mathbf{V}_i^{DVE}$ are, respectively, the contributions of the mass diffusion, thermal diffusion, and diffusion of vibrational energy, $\mathbf{q}^{HC}$, $\mathbf{q}^{MD}$, $\mathbf{q}^{TD}$, and $\mathbf{q}^{DVE}$ are, respectively, the energy fluxes associated with the heat conductivity of translational and rotational degrees of freedom (Fourier flux), mass diffusion, thermal diffusion, and vibrational energy transfer. The algorithm for calculating the transport coefficients was developed in [15].

NUMERICAL PROCEDURE

In the present work, we use a software package ANSYS Fluent, which allows us to simulate reacting gas mixture flows taking into account the transport processes. Our aim is to use the built-in model and computational capabilities of the package for numerical simulations of state-to-state kinetics.

It is worth mentioning that the ANSYS Fluent model does not account for the deviation from equilibrium over the internal degrees of freedom and, in particular, for vibrational excitation. In order to take into account the non-equilibrium vibrational distributions, the molecules at various vibrational levels are modeled as independent chemical species of the gas mixture. This representation allows us to introduce the VT process (2) so that the energy transitions are interpreted by the solver as chemical reactions. More details about implementing the production terms in the right-hand sides of Eqs. (3)-(4) and including the effect of kinetic processes to the total energy of the mixture can be found in [18].

Detailed analysis of the original set of equations (3)-(7) and physical model of the chosen flow-solver shows that this model does not include terms that describe the diffusion of vibrational energy:

$$\mathbf{V}_i^{DVE} = -n\left(\frac{n_m}{D_{mm}} + \frac{n_a}{D_{ma}}\right)^{-1} \nabla \ln \frac{n_i}{n_m}, \tag{13}$$

$$\mathbf{q}^{DVE} = \sum_i \left(\frac{5}{2}k_B T + \langle\varepsilon^i\rangle_{rot} + \varepsilon_i\right) n_i \mathbf{V}_i^{DVE}. \tag{14}$$

Here D_{mm} and D_{ma} are the multi-component diffusion coefficients for each molecule and atom, and $\langle\varepsilon^i\rangle_{rot}$ is the mean rotational energy. The terms V_i^{DVE} and q^{DVE} are introduced as source terms into the equations of energy conservation

and species mass conservation for the simulation of a 1D flow behind the shock wave in dissociating oxygen. In the simulations of the axisymmetric 2D flow of nitrogen around a cone, the terms V_i^{DVE} and q^{DVE} were not included yet due to computational difficulties.

The system of equations solved by the flow solver does not take into account the relaxation pressure p_{rel} included in the viscous stress tensor (see Eq. (10)). As is shown in [26], the contribution of relaxation pressure is small, so we assume that $p_{rel} = 0$ in our simulations. The shear viscosity η, bulk viscosity ζ and thermal conductivity coefficient λ are calculated by using built-in functions of the ANSYS Fluent. The mass and thermal diffusion fluxes are also computed with the use of internal solver functions, whereas, the missing terms V_i^{DVE} and q^{DVE} are calculated by user-defined functions.

The numerical simulation is performed with a density-based solver (specially developed for supersonic and hypersonic flows) with an implicit first-order upwind scheme. The fluxes through the control volume faces are calculated by the AUSM solver [27].

RESULTS AND DISCUSSION

In this section we report the results obtained for two problems solved numerically:

1. 2D N_2/N mixture flow around a cone;
2. 1D O_2/O mixture flow behind a plane shock wave.

In the first test case, the numerical calculations are performed for the N_2/N mixture flow near the cone with the half-angle $\delta = 75°$ for the following free-stream conditions: $M_\infty = 5.565$, $T_\infty = 1416$ K, $\rho_\infty = 0.0437$ kg/m^3, $n_m/n = 1$, $n_a/n = 0$, and cone diameter $d = 4$ cm. The vibrational level populations ahead of the shock have the form of the Boltzmann distribution with the temperature $T = T_\infty$. These free-stream conditions correspond to the experimental "conditions N_2 2" in [28].

To simulate the flow around the cone, a structured hexahedral grid refined toward the cone for resolving the boundary layer is constructed (see Fig. 1a). The body surface is assumed to be a non-catalytic wall, i.e., the normal gradient of each species mass fraction at the wall is zero. The wall is assumed to be isothermal at $T_w = 300$ K. The no-slip velocity condition and zero normal pressure gradient are applied at the cone.

The gas temperature and mass fraction variations obtained in the numerical simulations near the cone are plotted in Figs. 1b,c. A bow shock wave is formed ahead of the cone with a stand-off distance Δ/d from the cone tip. We can notice a jump of the temperature (Fig. 1b) and then T decreases due to TV transitions and dissociation. With the distance from the symmetry axis, the gas temperature diminishes in response to the decrease in the shock intensity. Figure 1c shows the monotonous growth of the atom mass fraction from 0 in the free stream to 0.068 close to the cone as a result of the finite rates of the kinetic processes.

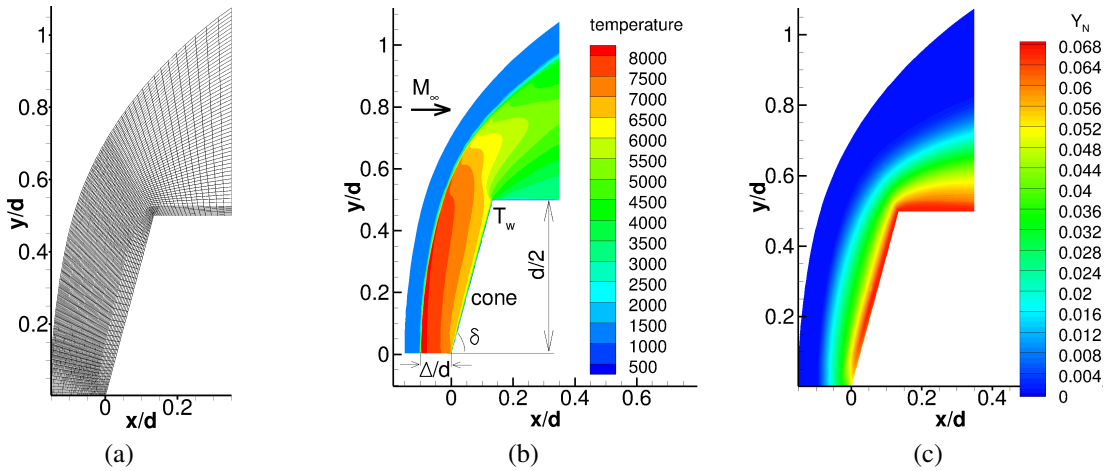

FIGURE 1. Mesh near the cone (**a**). Distribution of the translational-rotational temperature T (**b**) and mass fraction of atoms (**c**).

The mass fractions of nitrogen molecules for different vibrational levels near the cone are given in Fig. 2. Non-monotonic variation of the populations for non-zero levels reflects a rapid increase in the populations due to TV vibrational excitation and then a decrease as a result of dissociation and deactivation of excited molecules.

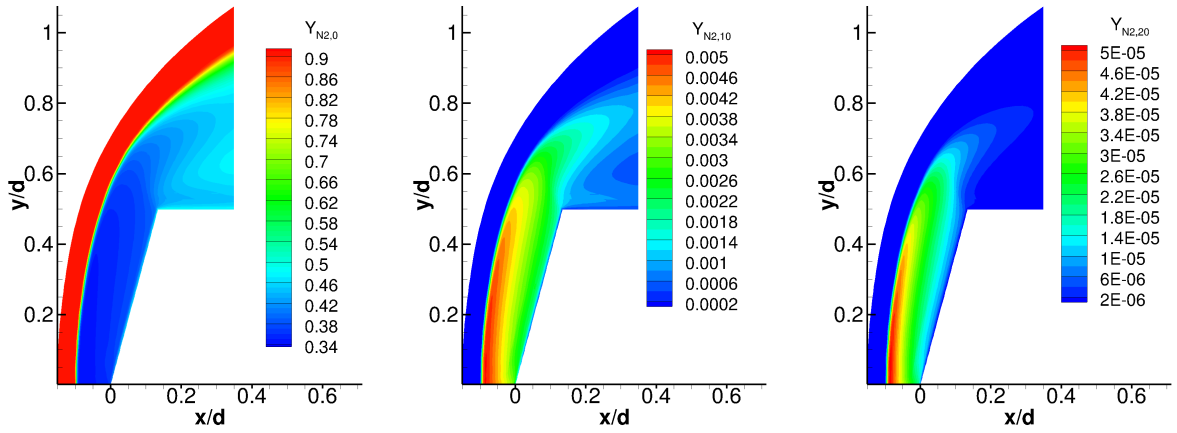

FIGURE 2. Distribution of mass fractions of molecules on the 0^{th} (**a**), 10^{th} (**b**) and 20^{th} (**c**) vibrational levels.

The calculated stand-off distance of the shock wave (Fig. 3a), the pressure coefficient (Fig. 3b), and the total heat flux (Fig. 3c) on the cone surface are compared with those measured in [28]. In our simulations, the state-specific rate coefficients of VT vibrational energy transitions are calculated using the generalized SSH-theory [29], the dissociation rates are described by the Treanor–Marrone (T–M) model with the use of different values of the parameter U: $U = D/6k_B$, $U = D/3k_B$, and $U = 3T$ (D is the dissociation energy). We also consider the case where the non-equilibrium factor of the T–M model is equal to unity, which corresponds to the thermal equilibrium dissociation rate coefficient described by the Arrhenius law ("Arrhenius" case in Fig. 3a). The parameters in the Arrhenius law are taken from [30] for $d = 4$ cm. The parameters [31] in the Arrhenius law were chosen in [28] for modeling the flow around a cone in the two-temperature approximation. Good agreement between experimental and numerical data for the heat flux was observed in [28]; therefore, the same parameters [31] were chosen in the present study to compare the state-to-state numerical results with the experimental measurements of the heat flux.

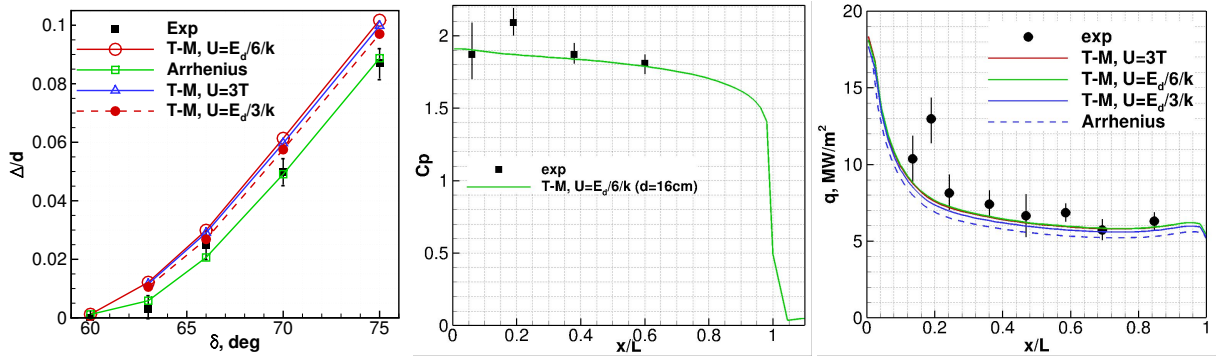

FIGURE 3. (**a**): Dimensionless stand-off distance of the shock wave for different values of the cone half-angle ($d = 4$ cm). (**b**): Pressure coefficient on the cone surface ($\delta = 70°$, $d = 16$ cm). (**c**): Total heat flux on the cone surface ($M_\infty = 5.725$, $T_\infty = 1239$ K, $\rho_\infty = 0.0266$ kg/m^3, $n_m/n = 1$, $n_a/n = 0$, $\delta = 70°$, $d = 8$ cm). All experimental data are taken from [28].

The behavior of the calculated shock wave stand-off distance qualitatively agrees well with experimental data (see Fig. 3a). The computations with the Arrhenius and T–M models of dissociation yield different stand-off distances, while variation of the parameter U in the T–M model has no significant impact on the numerical solution. The param-

eters in the equilibrium dissociation rate coefficients (Arrhenius law) can significantly affect the numerical solution, including the shock wave stand-off distance.

In the experiments [28], the pressure transducers and thermocouples were mounted along the cone hypotenuse L. The X coordinate given in Fig. 3b,c is the coordinate along the cone hypotenuse, so $x/L = 0$ corresponds to the cone tip and $x/L = 1$ to the trailing edge. The computed pressure coefficient agrees well with the experimental data, excluding the point $x/L = 0.2$. The heat flux given in Fig. 3c is also in good agreement with the experiment. Using of the Arrhenius law yields the lowest heat flux among all considered cases. The reason is that dissociation in the "Arrhenius" case proceeds faster than in the case of the T–M model. Thus, more energy is spent and the heat flux on the surface should be smaller.

In the second test case, we consider the flow of the O_2/O mixture in the relaxation zone behind a plane shock wave under the following free-stream condition: $T_\infty = 299$ K, $p_\infty = 1$ Torr, $v_\infty = 3400$ m/sec, $n_m/n = 1$, and $n_a/n = 0$. This condition corresponds to the experiment carried out in [32]. In this case, the diffusion of vibrational energy is taken into account.

In our calculations, we use different models for the dissociation rate coefficients: 1) the Treanor–Marrone model with the constant $U = D/6k_B$, 2) a modification of the Park model [33]. In order for the Park model to be used in the state-to-state approach, instead of the single vibrational temperature T_v, we define vibrational temperatures corresponding to each vibrational state of a molecule. It allows us to generalize the Park model for the case of non-Boltzmann vibrational distributions. The parameters involved in the Park and T–M models (for the thermal equilibrium dissociation rate coefficients) are taken from [34].

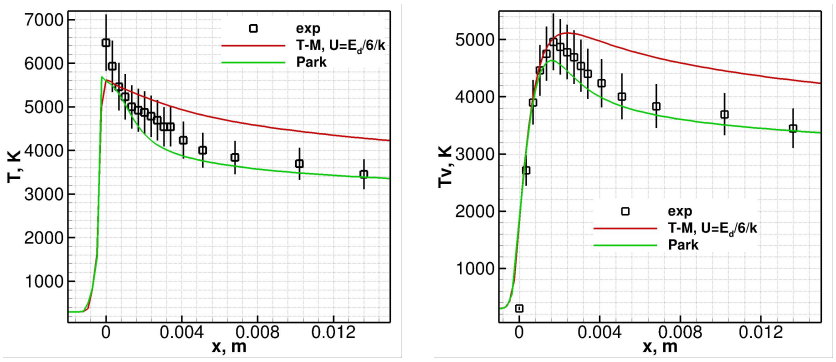

(a) (b)

FIGURE 4. Gas temperature (**a**) and vibrational temperature (**b**) in the O_2/O mixture as functions of x. Comparison with experiments [32].

Figure 4 present a comparison of the calculated gas temperature and temperature of the first vibrational level

$$T_1 = \frac{\varepsilon_1}{k_B \ln(n_0/n_1)}$$

with the temperature of the oxygen mixture and vibrational temperature T_v measured in [32]. Experimental determination of vibrational temperature was based on comparisons of the measured and calculated oxygen absorption characteristics and verified assumption that the harmonic oscillator model adequately describes the energy spectrum of molecules on the low vibration levels. Further, using the measured vibrational temperature, the gas temperature was defined numerically. As we can see, the numerical simulations yield significantly underestimated values of the gas temperature at the beginning of the relaxation zone, but the discrepancy reduces with the distance from the shock front. The modified Park model provides a more efficient dissociation process compared to the T–M model and, thus, yields better agreement with the measured temperature; the calculated value of T falls within the limits of the experimental error (see Fig. 4a).

The best agreement for the location of the vibrational temperature maximum is ensured by the T–M model (Fig. 4b). However, as x increases, the T–M model yields slower relaxation and a higher value of vibrational temperature. Satisfactory agreement for the calculated and measured vibrational temperature in the deactivation zone is provided by the modified Park model.

CONCLUSIONS

A method of non-equilibrium flow simulations on the basis of the state-to-state approach using the commercial flow solver ANSYS Fluent is proposed. This method takes advantages of broad solver capabilities, which are supplemented by the user's code for calculating the rate coefficients of energy transitions, dissociation reaction, and additional source terms in the energy conservation equation required for the correct description of state-to-state kinetics.

The proposed numerical tool was used for various computations to compare the numerical solutions with available experimental data. The calculations show that the choice of the dissociation model is important and the results strongly depend on the model used in computations. Computations with the Arrhenius model of dissociation provide better agreement with the experimental data on the shock stand-off distance in the case of the nitrogen mixture flow around the cone. The total heat flux on the cone surface obtained for different dissociation models is within the experimental error. In the case of the oxygen mixture flow, the proposed modification of the Park model yields the gas temperature and vibrational temperature close to the experimental ones behind the plane shock wave.

These results allow us to conclude that ANSYS Fluent can be used for further numerical studies of high-enthalpy gas flows on the basis of the state-to-state description taking into account state-specific transport phenomena.

ACKNOWLEDGMENTS

This study was supported by the Russian Science Foundation (project No. 15-19-30016). O. Kunova acknowledges that she is employed by the Saint-Petersburg State University within the framework of post-doctoral fellowship (No. 6.50.2522.2013).

REFERENCES

[1] F. Lordet, J. Meolans, A. Chauvin, and R. Brun, Shock Waves **4**, 299–312 (1995).
[2] I. Adamovich, S. Macheret, J. W. Rich, and C. E. Treanor, AIAA Journal **33**, 1064–1069 (1995).
[3] B. D. Shizgal and F. Lordet, J. Chem. Phys. **104**, 3579–3597 (1996).
[4] G. Colonna, M. Tuttafesta, M. Capitelli, and D. Giordano, J. Thermophys. Heat Transfer **14**, 455–456 (2000).
[5] I. Armenise, M. Capitelli, and C. Gorse, J. Thermophys. Heat Transfer **10**, 397–405 (1996).
[6] I. Armenise, F. Esposito, and M. Capitelli, Chem. Phys. **336**, 83–90 (2007).
[7] D. Giordano, V. Bellucci, G. Colonna, M. Capitelli, I. Armenise, and C. Bruno, J. Thermophys. Heat Transfer **11**, 27–35 (1997).
[8] J. G. Kim and I. D. Boyd, Chem. Phys. **415**, 237–246 (2013).
[9] M. Panesi, A. Munafò, T. E. Magin, and R. L. Jaffe, Phys. Rev. E **90**, p. 013009 (2014).
[10] E. Kustova, A. Aliat, and A. Chikhaoui, Chem. Phys. Lett. **344**, 638–646 (2001).
[11] A. Aliat, A. Chikhaoui, and E. Kustova, Phys. Rev. E **68**, p. 056306 (2003).
[12] E. Josyula, J. M. Burt, E. Kustova, and P. Vedula, AIAA Paper 2014–0864 (2014).
[13] E. Nagnibeda and E. Kustova, *Nonequilibrium Reacting Gas Flows. Kinetic Theory of Transport and Relaxation Processes* (Springer, Berlin, 2009).
[14] E. Kustova and E. Nagnibeda, Chem. Phys. **233**, 57–75 (1998).
[15] E. Kustova, Chem. Phys. **270**, 177–195 (2001).
[16] E. Kustova, E. Nagnibeda, I. Armenise, and M. Capitelli, J. Thermophys. Heat Transfer **16**, 238–244 (2002).
[17] O. Kunova, E. Kustova, M. Mekhonoshina, and E. Nagnibeda, Chem. Phys. **463**, 70–81 (2015).
[18] O. Kunova, G. Shoev, and A. Kudryavtsev, Thermophys. Aeromech. **24** (2017).
[19] S. V. Kirilovskiy, A. A. Maslov, T. V. Poplavskaya, and I. S. Tsyryul'nikov, Tech. Phys. **60**, 645–655 (2015).
[20] N. V. Petrov, S. V. Kirilovskiy, T. V. Poplavskaya, and G. V. Shoev, Tech. Phys. Lett. **42**, 695–698 (2016).
[21] G. Shoev, Y. Bondar, G. Oblapenko, and E. Kustova, Thermophys. Aeromech. **23**, 159–171 (2016).
[22] G. Shoev and Y. Bondar, "Numerical study of non-equilibrium gas flows with shock waves by using the navier–stokes equations in the two-temperature approximation," in *Proceedings of 18th International Conference on Methods of Aerophysical Research (ICMAR 2016), June 27 – July 3, 2016, Perm, Russia*, AIP Conf. Proc. (American Institute of Physics, in press).
[23] D. Paterna, R. Monti, R. Savino, and A. Esposito, J. Spacecraft Rockets **39**, 227–236 (2002).
[24] I. Armenise, M. Barbato, M. Capitelli, and E. Kustova, J. Thermophys. Heat Transfer **20**, 465–476 (2006).
[25] E. Kustova, E. Nagnibeda, T. Alexandrova, and A. Chikhaoui, Chem. Phys. **276**, 139–154 (2002).

[26] E. Kustova, "On the role of bulk viscosity and relaxation pressure in non-equilibrium flows," in *Proceedings of the 26th International Symposium on Rarefied Gas Dynamics*, AIP Conf. Proc., Vol. 1084, edited by T. Abe (American Institute of Physics, Melville, NY, 2008), pp. 807–812.
[27] M. S. Liou and C. J. S. Jr., J. Comput. Phys. **107**, 23–39 (1993).
[28] I. A. Leyva, "Shock detachment processes on cones in hypervelocity flows," Ph.D. thesis, California Institute of Technology 1999.
[29] R. Schwartz, Z. Slawsky, and K. Herzfeld, J. Chem. Phys. **20**, 1591–1599 (1952).
[30] J. N. Moss, G. A. Bird, and V. K. Dogra, AIAA Paper 88–0081 (1988).
[31] C. Park, AIAA paper 85-0247 (1985).
[32] L. B. Ibraguimova, O. P. Shatalov, and Y. V. Tunik, "Equilibrium and non-equilibrium rate constants of oxygen dissociation at high temperatures," in *Proceedings of the 28th International Symposium on Rarefied Gas Dynamics*, AIP Conf. Proc., Vol. 1501 (American Institute of Physics, Melville, NY, 2012), pp. 1094–1101.
[33] C. Park, J. Thermophys. Heat Transfer **3**, 233–244 (1989).
[34] I. E. Zabelinskii, L. B. Ibraguimova, and O. P. Shatalov, Fluid Dynamics **45**, 485–492 (2010).